CHEMISTRY
A EUROPEAN JOURNAL

DOI: 10.1002/chem.200801090

Intracellular Uptake and Photodynamic Activity of Water-Soluble [60]- and [70]Fullerenes Incorporated in Liposomes

Yuki Doi,[a, b] Atsushi Ikeda,*[a] Motofusa Akiyama,[a] Mai Nagano,[a] Tamami Shigematsu,[a] Takuya Ogawa,[c] Tatsuo Takeya,[c] and Takeshi Nagasaki[b]

Abstract: Water-soluble fullerenes have attracted attention as promising compounds that have been used to forge new paths in the field of photobiochemistry. To prepare water-soluble fullerenes, we employed lipid-membrane-incorporated fullerenes ($LMIC_x$; $x=60$ or 70) by using the fullerene exchange method from a γ-cyclodextrin (γ-CD) cavity to vesicles. $LMIC_{60}$ have low toxicity in the dark and engender cell death by photoirradiation ($\lambda>350$ nm). Furthermore, the photodynamic activity of $LMIC_{70}$ is 4.7-fold that of $LMIC_{60}$ for the same photon flux ($\lambda>400$ nm). One of the reasons for the higher phototoxicity of $LMIC_{70}$ is the higher generation of singlet oxygen ($^1O_2$) in $LMIC_{70}$ than in $LMIC_{60}$. The difference between $LMIC_{60}$ and $LMIC_{70}$ is considered to be simply derived from the amount of light absorption in the 400–700 nm region that is suitable for photodynamic therapy (PDT). To the best of our knowledge, this is the first case in which biological activity of C_{70} and its derivatives toward HeLa cells has been assayed.

Keywords: biological activity · fullerenes · liposomes · photochemistry · photodynamic activity

Introduction

Photodynamic therapy (PDT) has been developed for cancer treatment over the last 40 years. It has been expanded as an emerging modality for the treatment of various cardiovascular, dermatological, and ophthalmic diseases.[1] Water-soluble C_{60}[2,3] and its derivatives[4] have recently received attention as potential photosensitizers because C_{60} is an efficient visible-light triplet sensitizer and is capable of high photoproduction of $^1O_2$ (energy transfer) and anion radicals (electron transfer).[5] However, fullerenes themselves are insoluble in water and polar solvents.[6] Several research efforts have attempted to solve this problem, for example, by introducing water-soluble substituents,[4] mixing with water-soluble polymers[3f,7] or lipid membranes (Bangham method),[8] and dissolving in γ-cyclodextrin (γ-CD)[9] or water-soluble calixarenes.[3a–b,10] Among these methods, we have selected lipid-membrane-incorporated fullerenes ($LMIC_x$, $x=60$ or 70; Scheme 1) as photosensitizers for three reasons: 1) unmodified fullerenes in vesicles can generate $^1O_2$ through energy transfer, or fullerene anion radicals by electron transfer, more efficiently than other chemically modified fullerene derivatives can;[3,5] 2) various vesicles with positively charged, negatively charged, nonionic, and zwitterionic surfaces can be prepared through selection of lipids such as phospholipids, aminolipids, and glycolipids, which might confer a function as a drug carrier;[11] and

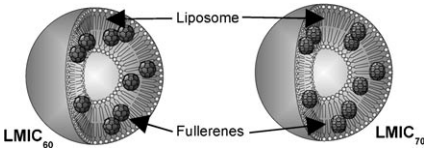

Scheme 1. Schematic illustration of $LMIC_{60}$ and $LMIC_{70}$.

[a] Y. Doi, Dr. A. Ikeda, Dr. M. Akiyama, M. Nagano, T. Shigematsu
Graduate School of Materials Science
Nara Institute of Science and Technology
Ikoma, Nara 630-0192 (Japan)
Fax: (+81) 743-72-6091
E-mail: aikeda@ms.naist.jp

[b] Y. Doi, Prof. T. Nagasaki
Department of Applied Chemistry and Bioengineering
Graduate School of Engineering, Osaka City University
3-3-138 Sugimoto, Sumiyoshi-ku, Osaka 558-8585 (Japan)

[c] Dr. T. Ogawa, Prof. T. Takeya
Graduate School of Biological Science
Nara Institute of Science and Technology
Ikoma, Nara 630-0192 (Japan)

Supporting information for this article is available on the WWW under http://dx.doi.org/10.1002/chem.200801090.

3) large vesicle formation is promising for enhanced permeability and retention (EPR) effects.[4a,12] Recently, we reported that various types of $LMIC_x$ with high C_{60} or C_{70} concentrations were able to be readily prepared in several hours or minutes by using the fullerene exchange method from the γ-cyclodextrin (γ-CD) cavity to vesicles.[3c–e] Furthermore, this method can be treated as a homogeneous system that requires no separation procedure, such as gel exclusion chromatography, for incorporated and insoluble fullerenes because nearly all of the C_{60} molecules are transferred from the γ-CD cavity to the lipid membranes to yield vesicle-incorporated fullerenes. The DNA photocleaving activity of $LMIC_{60}$ depends on the surface charges of the vesicles. In particular, the photocleaving activity of cationic $LMIC_{60}$ is considerably higher than that of the C_{60}•γ-CD complex. In this study, we assayed the biological activities of $LMIC_{60}$ and $LMIC_{70}$ under visible light irradiation.

Results and Discussion

Characterization of $LMIC_x$: To examine the effect of liposome surface density, we prepared three types of $LMIC_{60}$ with different surface charges. To investigate the effect of using different fullerenes, cationic $LMIC_{70}$ were also prepared with the same concentration of liposomes and fullerenes as in $LMIC_{60}$. All $LMIC_{60}$ and $LMIC_{70}$ were prepared by using an exchange reaction between the liposomes and the C_{60}•γ-CD complex or the C_{70}•γ-CD complex[9] by heating at 80 °C for 2 h or at 30 °C for 1 min, as described in previous reports.[3c,e]

Size distributions of the liposomes were studied by using dynamic light scattering (DLS) analyses. Table 1 shows the average diameters of all the liposomes before and after the exchange reaction of C_{60} and C_{70}. The average diameters after the exchange reactions in all $LMIC_{60}$ and $LMIC_{70}$ were around 100 nm.

Table 1. Average particle sizes determined by using a light-scattering method at 25 °C before and after the exchange reaction.

	Lipids		Average particle size [nm][a] Before fullerene addition	After fullerene addition
$LMIC_{60}$	**1**	**2**	95 ± 2	117 ± 1
$LMIC_{60}$	**1**	–	72 ± 14	103 ± 9
$LMIC_{60}$	**1**	**3**	91 ± 1	93 ± 1
$LMIC_{70}$	**1**	**2**	91 ± 33	80 ± 27

[a] Each of these experiments was performed three times. The reported values of particle sizes are averages of these separate runs.

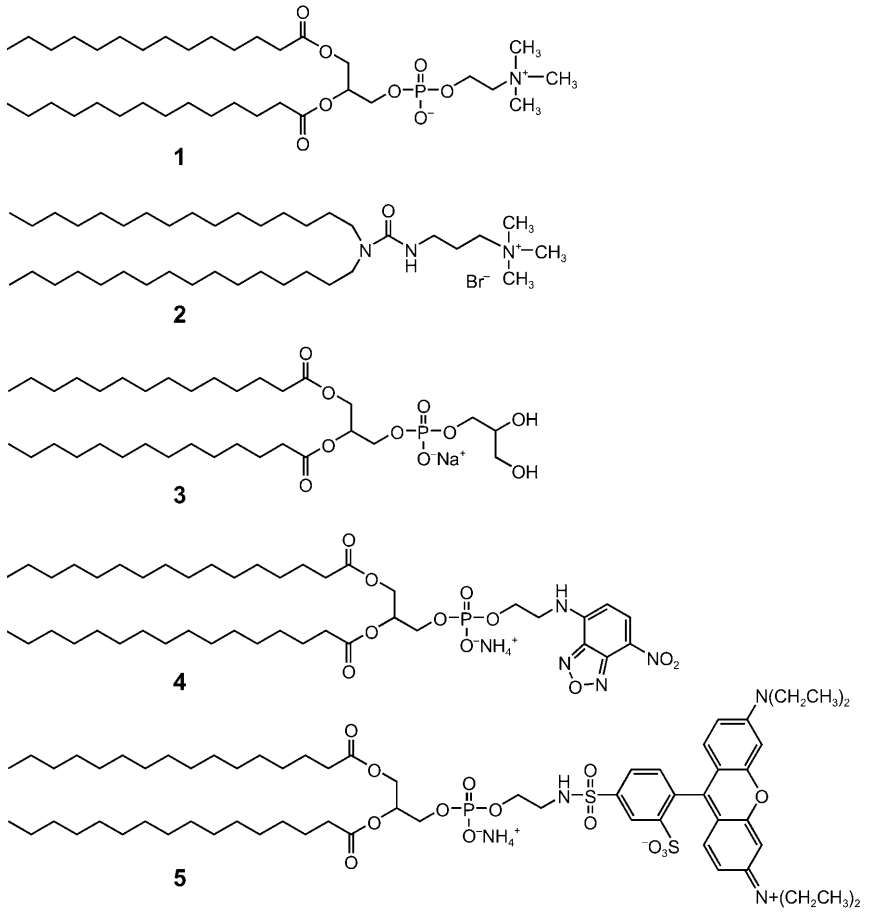

Intracellular uptake and localization of liposomes: To evaluate the intracellular uptake of the liposomes by HeLa cells, fluorochrome-labeled liposomes were prepared using 7-nitrobenz-2-oxa-1,3-diazole (NBD)-conjugated lipids (**4**) without fullerenes, because fullerenes act as quenchers. The cells were incubated with NBD-labeled liposomes at a lipid concentration of 50 μM for 24 h. Figure 1 clearly indicates intracellular uptake of liposomes was only observed for cationic liposome treated cells (Figure 1a and d). No fluorochrome signals were detected for the neutral and anionic liposome treated cells (Figure 1e and f). Effects of the surface density were consistent with those described in previous reports.[3f,13]

To elucidate the mechanism of the uptake of liposomes, the effect of low temperature was evaluated because endocytotic processes are known to be inhibited at low temperatures. HeLa cells were incubated with

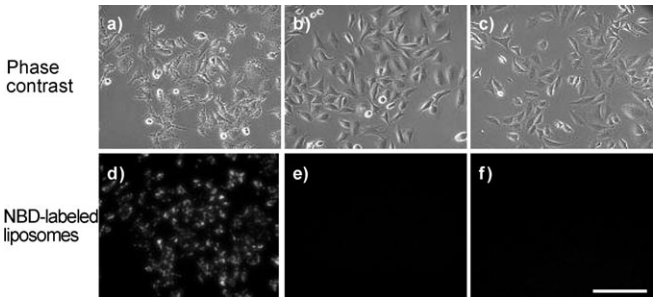

Figure 1. Phase contrast (a–c) and fluorescence (d–f) images of HeLa cells after NBD-labeled liposome treatment for 24 h. a) and d) NBD-labeled liposomes of **1+2+4**; b) and e) NBD-labeled liposomes of **1+4**; c) and f) NBD-labeled liposomes of **1+3+4**. The scale bar indicates 200 μm.

fluorochrome-labeled liposomes for 1 h at 37 or 4 °C. As a result, the liposome uptake was notably inhibited at 4 °C compared with that at 37 °C (Figure 2). Furthermore, we

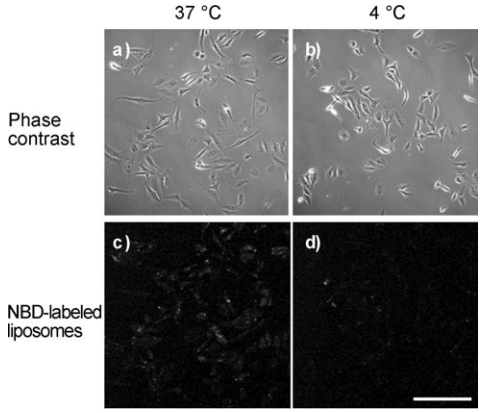

Figure 2. Inhibition of liposome uptake by low temperature. HeLa cells were incubated with NBD-labeled liposomes for 1 h at 37 (a, c) or 4 °C (b, d). Fluorescence images were obtained by using confocal laser scanning microscopy. Phase contrast (a, b) and cationic liposomes labeled with NBD (c, d). The scale bar indicates 200 μm.

stained lysosomes with LysoTracker Green and compared them with the localization of cationic liposome, because normal cellular trafficking usually involves endocytosed particles being directed to lysosomes. The cells were incubated with fluorochrome-labeled cationic liposomes that had been prepared by using rhodamine B-conjugated lipids (**5**) for 1 h at 37 °C. After incubation, the cells were further cultured and the localization of fluorochrome-labeled liposomes was monitored. As shown in Figure 3, cationic liposomes accumulated in lysosomes until 6 h after incubation. These data indicate that cationic liposomes of **1+2** internalize into the cells by means of the endocytotic processes and localize to lysosomes.

Photodynamic activity of LMIC$_{60}$: Three types of LMIC$_{60}$ with different surface charges were evaluated in culture for photodynamic activity toward HeLa cells. The cells were incubated with LMIC$_{60}$ ([C$_{60}$] = 5 μM) for 24 h in the dark. The

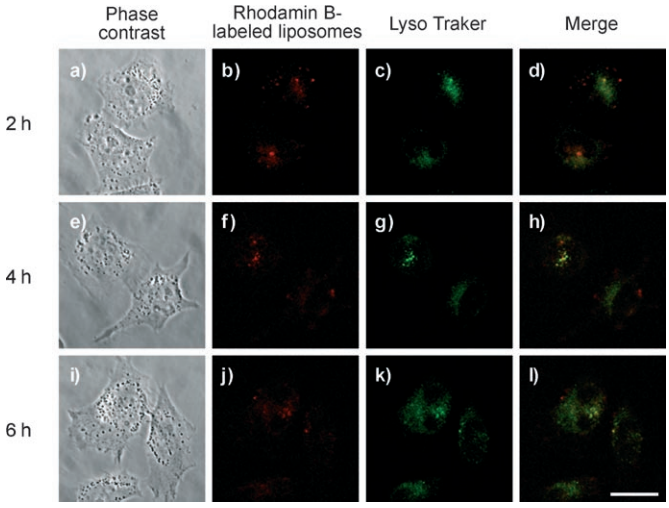

Figure 3. Localization of cationic liposomes in HeLa cells. The cells were incubated with rhodamine B-labeled cationic liposomes for 1 h at 37 °C. After incubation, the cells were further cultured for 2 (a–d), 4 (e–h), or 6 h (i–l). Lysosomes were visualized by staining with LysoTracker Green for 1 h before observation and were observed by using confocal laser scanning microscopy: phase contrast (a, e, and i), cationic liposomes labeled with rhodamine B (b, f, and j), staining with LysoTracker Green (c, g, and k), and merged image (d, h, and l). The scale bar indicates 20 μm.

cells treated with LMIC$_{60}$ of **1+2** had abnormal shapes after light irradiation (350–500 nm), whereas treatments with LMIC$_{60}$ of **1** or **1+3** induced no apparent change (Figure 4a–c). It is thought that this morphological change probably re-

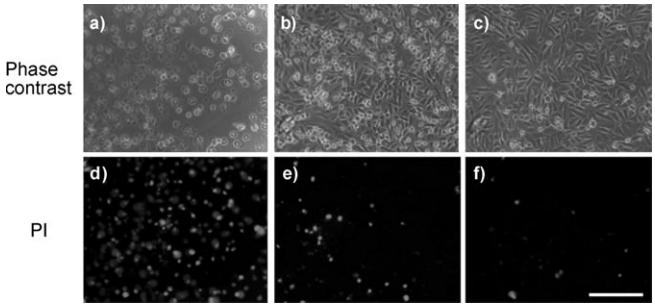

Figure 4. Photodamage from LMIC$_{60}$ in HeLa cells. The cells were exposed to light (350–500 nm) for 2 h at 19 mW cm^{-2} and observed by using microscopy: phase contrast images (a–c) and exclusion of propidium iodide (d–f). a) and d) LMIC$_{60}$ of **1+2**. b) and e) LMIC$_{60}$ of **1**. c) and f) LMIC$_{60}$ of **1+3**. The scale bar indicates 200 μm.

sulted from cell death because the cell was unable to exclude propidium iodide (PI) (Figure 4d–f). The quantitative data of cell cytotoxicity are shown in Table 2. 85 % of cells were stained with PI by treatment with LMIC$_{60}$ of **1+2** in combination with light irradiation, but few cells were stained by the neutral and anionic LMIC$_{60}$ (4 % for **1** and 1 % for **1+3**). LMIC$_{60}$ showed no cytotoxicity to the cells in the dark after 24 h incubation (Table 2; 0.0–1.3 %). These results are consistent with those for the intracellular uptake of fluoro-

Table 2. Percentages of cells stained with PI. HeLa cells treated with $LMIC_{60}$ of **1+2**, **1**, and **1+3** and $LMIC_{70}$ before and after 19 mW cm^{-2} light irradiation over $\lambda = 350$ nm for 2 h at 35 °C and 57 mW cm^{-2} light irradiation over $\lambda = 400$ nm for 1 h at 35 °C.

	Lipids		Fullerene	Light λ [nm]	Percentages of cells stained with PI [%][a]
$LMIC_{60}$	**1**	**2**	C_{60}	>350	84.8±4.5
$LMIC_{60}$	**1**	**2**	C_{60}	–	0.1±0.1
$LMIC_{60}$	**1**	–	C_{60}	>350	3.8±2.4
$LMIC_{60}$	**1**	–	C_{60}	–	1.3±1.0
$LMIC_{60}$	**1**	**3**	C_{60}	>350	0.9±0.6
$LMIC_{60}$	**1**	**3**	C_{60}	–	0.0±0.0
$LMIC_{60}$	**1**	**2**	C_{60}	>400	18.9±8.8
$LMIC_{70}$	**1**	**2**	C_{70}	>400	89.0±4.7
$LMIC_{70}$	**1**	**2**	C_{70}	–	1.1±0.2

[a] Each of these experiments was performed three times. The reported values of particle sizes are averages of these separate runs.

chrome-labeled liposomes, indicating intracellular $LMIC_{60}$ can act as a photosensitizer.

Comparison of photodynamic activity between $LMIC_{60}$ and $LMIC_{70}$: As mentioned above, $LMIC_{60}$ with the cationic surface efficiently engender cell death by photoirradiation, compared with $LMIC_{60}$ with a neutral or anionic surface. Therefore, we prepared $LMIC_{70}$ with a cationic surface to clarify the difference between C_{60} and C_{70}. After incubation with 5 μM fullerenes of $LMIC_{60}$ or $LMIC_{70}$ for 24 h, the cells were exposed to light with a wavelength of 400–740 nm for 45 and 60 min each. The power of the light at the cellular level was 57 mW cm^{-2}. The cells treated with $LMIC_{70}$ had abnormal shape (Figure 5k and l) and were stained with PI after light irradiation (Figure 5n and o), whereas treatments with $LMIC_{60}$ hardly induced apparent change (Figure 5b and c). Table S1 in the Supporting Information shows the percentages of cells stained with PI by $LMIC_{60}$ and $LMIC_{70}$ as a function of irradiation time. No cytotoxicity was observed for $LMIC_{60}$ and $LMIC_{70}$ without light exposure (Table 2; 0.1 and 1.1%, respectively). The difference in build-up curves between $LMIC_{60}$ and $LMIC_{70}$ was derived simply from amounts of light absorption in the 400–700 nm region (Figure S1 in the Supporting Information); this is explained later. Quantitative data of the percentage of cells stained with PI are shown in Table 2: around 89% of cells were stained with PI by treatment with $LMIC_{70}$ in combination with light irradiation for 60 min, but only a few cells were stained when using $LMIC_{60}$ (19%). These results indicate the photodynamic activity of $LMIC_{70}$ is much higher than that of $LMIC_{60}$ by photoirradiation at a wavelength longer than 400 nm.

Analysis of the mode of cell death induced by $LMIC_{60}$ and $LMIC_{70}$: To examine the mode of cell death induced by cationic $LMIC_{60}$ and $LMIC_{70}$, cell-surface-exposed phosphatidyl serine, which is present in the earlier stages of apoptosis, was visualized by using fluorescein isothiocyanate (FITC)-conjugated annexin V. By combining FITC-conjugated annexin V with PI, the different labeling patterns can be used to identify the different cell fractions; that is, PI-negative/annexin V-negative viable cells, PI-negative/annexin V-positive early apoptotic cells, PI-positive/annexin V-positive late apoptotic, and/or necrotic cells.[14] Figure 5n and q show cells stained with annexin V were stained incompletely with PI by treatment with $LMIC_{70}$ in combination with light irradiation for 45 min, which suggests that $LMIC_{70}$ induced early apoptosis at least in part.[14] Furthermore, the cells treated with $LMIC_{60}$ were stained with only annexin V after light irradiation, which indicates that these cells undergo early apoptosis (Figure 5e and h), suggesting that $LMIC_{60}$ also has the potential to induce apoptosis when combined with light irradiation for 45 min.

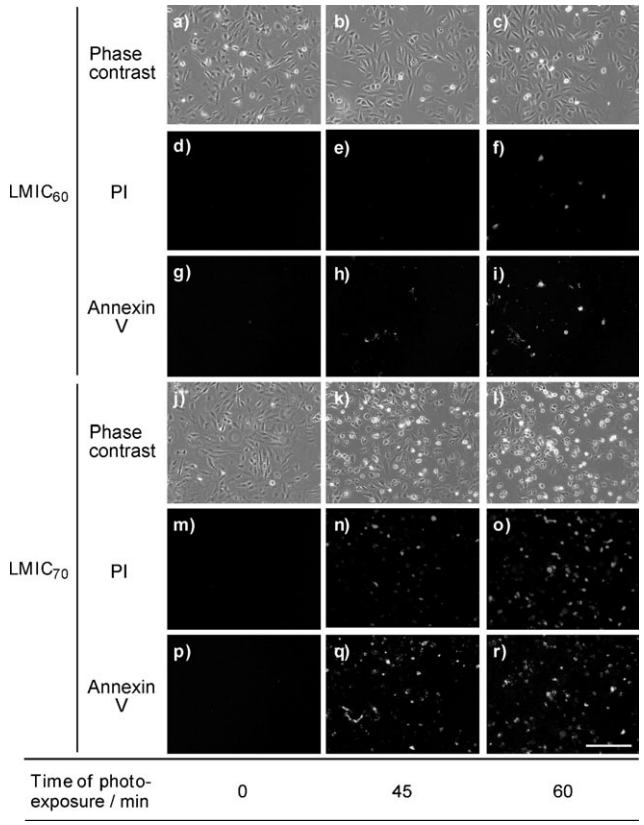

Figure 5. Photodamage from $LMIC_{60}$ and $LMIC_{70}$ in HeLa cells as detected using phase contrast images (a–c and j–l) and by fluorescence microscopy using propidium iodide (d–f and m–o) and FITC-conjugated annexin V (g–i and p–r) and fluorescent staining after 57 mW cm^{-2} light irradiation (400–740 nm) at 35 °C. Light irradiation for a), d), g), j), m), and p) was 0 min; that for b), e), h), k), n), and q) was 45 min; and that for c), f), i), l), o), and r) was 60 min. The scale bar indicates 200 μm.

Singlet oxygen detection by using a chemical method: The photosensitizer is excited by visible light. An excited-state energy is then transferred from the triplet state of the sensitizer to the ground state of the molecular oxygen producing the cytotoxic species $^1O_2$.[15] Therefore, the photodynamic activity of the photosensitizers is dependent on the generation ability of $^1O_2$. We confirmed $^1O_2$ generation by using a chemical method using 9,10-anthracenedipropionic acid disodium salt (ADPA)[16] as a detector to clarify the reason for the difference in biological activities between $LMIC_{60}$ and $LMIC_{70}$.[17] Figure 6 shows the decrease in absorbance at

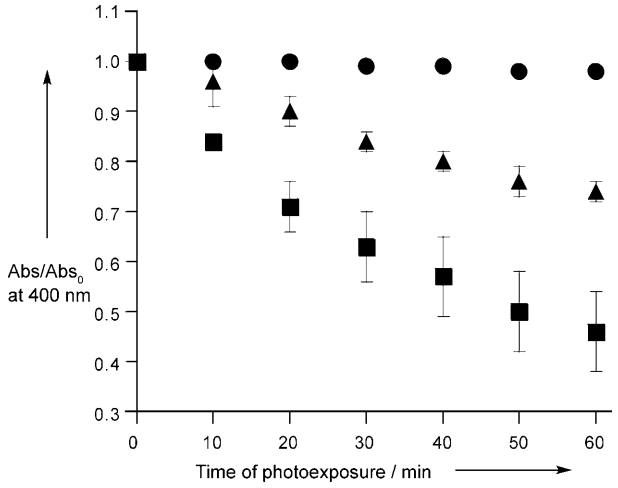

Figure 6. Time-dependent bleaching of 9,10-anthracenedipropionic acid disodium salt (ADPA) caused by singlet oxygen generated a) without $LMIC_x$ (●) and b) with $LMIC_{60}$ of **1** (▲), and c) with $LMIC_{70}$ of **1** (■). The change in ADPA absorption at 400 nm upon photoirradiation (440 nm, 0.6 mW cm^{-2}) was monitored as a function of time (Abs_0: initial absorbance). [ADPA] = 134 μM, [lipids] = 146 μM; under an oxygen atmosphere; 25 °C. Each experiment was repeated three times.

400 nm (absorption maximum for ADPA) for a lipid concentration of 146 μM for $LMIC_{60}$ and $LMIC_{70}$ of **1** as a function of the time of light exposure. Time-dependent bleaching of ADPA was shown to occur severely for $LMIC_{70}$ compared with that for $LMIC_{60}$, which indicates the generation of $^1O_2$ in $LMIC_{70}$ is higher than that in $LMIC_{60}$. Furthermore, we have reported the plasmid DNA photocleavage ability of $LMIC_{70}$ is greater than that of $LMIC_{60}$ (the respective percentages of form II (nicked DNA) and form III (linear DNA) are 92 and 26% under visible light irradiation ($\lambda_{ex} > 350$ nm) for 2 h).[3e] From these two findings, the difference between $LMIC_{60}$ and $LMIC_{70}$ is derived simply from amounts of light absorption in the 400–700 nm region (Figure S1). $LMIC_{70}$ is anticipated to be a much more potent photosensitizer than conventional photoreactors.

Conclusion

The results of this study show that the $LMIC_{60}$ of **1+2** with a cationic surface shows a low dark toxicity that engenders cell death by photoirradiation at a wavelength of 350–500 nm. The photodynamic activity of the $LMIC_{60}$ of **1+2** is much higher than that of the $LMIC_{60}$ of **1** or **1+3**. These results agree very well with those for the intracellular uptake of $LMIC_{60}$. However, the photodynamic activity of the $LMIC_{60}$ of **1+2** degraded remarkably by photoirradiation at a wavelength over 400 nm, which indicates that the $LMIC_{60}$ were activated mainly by light in the 350–400 nm region. On the other hand, the $LMIC_{70}$ have low toxicity in the dark and engender cell death by photoirradiation at wavelengths of 400–740 nm. The photodynamic activity of $LMIC_{70}$ is 4.7-fold that of $LMIC_{60}$ for the same photon flux (>400 nm). To the best of our knowledge, we have demonstrated photoinduced cell death using C_{70} for the first time. These findings have important implications for various applications in biological, medicinal, and materials chemistry because materials-incorporated C_{70} can be prepared easily by using the exchange method. Applications of these systems are being studied in our laboratories.

Experimental Section

General: UV-visible spectra were obtained by using a UV-2550 spectrophotometer (Shimadzu Corporation). Size distributions were measured by using a DLS-6000HL instrument (Otsuka Electronics Co. Ltd.). Light irradiation was performed by using a xenon lamp (MAX-301, 300 W; Asahi Spectra Co. Ltd.) equipped with a purpose-built mirror module (350–500 nm; Asahi Spectra Co. Ltd.) and a long-pass filter with cut-off at 350 nm (Asahi Spectra Co. Ltd.) for photoirradiation over 350 nm wavelength, or a VIS mirror module (385–740 nm; Asahi Spectra Co. Ltd.) and a long-pass filter with cut-off at 400 nm (Asahi Spectra Co. Ltd.) for photoirradiation over 400 nm wavelength. Fluorescence microscopy was performed with an inverted Axiovert 135M, equipped with an AxioCam CCD camera and AxioVision 3.0 software (Carl Zeiss Inc.). The following sets of filters were used: PI (BP546, FT580, and LP 590) and NBD and FITC (450–490, FT 510, and 515–565). In some experiments, fluorescence images were obtained by using a confocal laser scanning microscope (LSM 410; Carl Zeiss Inc.). The following lasers and sets of filters were used: rhodamine B (He–Ne laser $\lambda = 543$ nm; NT80/20-543 and LP 570) and NBD and LysoTracker Green (Ar laser $\lambda =$ 488 nm; FT 510 and LP515).

Materials: Compound **2** was prepared as described in a previous paper.[18] Dimyristoylphosphatidylcholine (**1**) and γ-CD were purchased from NOF Corp. (Tokyo, Japan) and Wako Pure Chemical Industries Ltd., respectively. Dimyristoylphosphatidylglycerol (**3**), NBD–dipalmitoylphosphatidylethanolamine (**4**), and rhodamine B–dipalmitoylphosphatidylethanolamine (**5**) were obtained from Avanti Polar Lipids Inc. (Birmingham, AL). C_{60} (>99.5%) and C_{70} (>95%) were bought from MER Co. (Tucson, AZ).

Preparation of liposomes: All liposomes were prepared through sonication of an aqueous dispersion of lipids with a cup-type sonicator at 50 W for 1 h at 40 °C. Each liposome was composed of **1** only, or **1** and cationic lipid **2** or anionic lipid **3** in a 9:1 molar ratio, respectively. NBD-conjugated lipid **4** (0.25 mol% relative to the total lipids) or rhodamine B-conjugated lipid **5** (0.025 mol% relative to the total lipids) were supplied to label the liposomes with fluorochromes.

Preparation of $LMIC_{60}$ and $LMIC_{70}$ by means of the fullerene exchange reaction: $LMIC_{60}$ were prepared by using an exchange reaction between the liposomes and the C_{60}•γ-CD complex[9b] by heating at 80 °C for 2 h, as described in previous work.[3c] Size distributions of the liposomes were studied by using DLS analyses. Final concentrations of the respective components were evaluated by using integral intensities of their ^{1}H NMR spectra, in which [γ-CD] = 1.02 mM, [C_{60}] = 0.10 mM, and [lipids] = 1.00 mM (γ-CD/C_{60}/lipids = 10.2:1:10). The initial concentration of C_{70} in the C_{70}•γ-CD complex, as determined by measuring the absorbance of the solution at 381 nm (a molecular extinction coefficient for the C_{70}•γ-CD complex of $\varepsilon_{381} = 3.80 \times 10^4$ dm^3 mol^{-1} cm^{-1}),[9b] was 0.20 mM in an aqueous solution (1.0 mL). After an aqueous solution of lipids (10 equiv of C_{70}) was added to the solution (1.0 mL, 2.00 mM), final concentrations of the respective components were evaluated by using integral intensities of the ^{1}H NMR spectrum,[19] in which [γ-CD] = 1.90 mM, [C_{70}] = 0.10 mM, and [lipids] = 1.00 mM (γ-CD/C_{70}/lipids = 19:1:10).

Cell culture: HeLa cells were maintained in CO_2-independent medium (Gibco BRL) supplemented with 10% fetal calf serum at 37 °C in 5% CO_2. The cells were seeded on 35 mm plates at a density of 3.4×10^5 cells per plate. After growing overnight, the cells were used for the experiments. For analysis of the uptake mechanism of liposomes, localization of

liposomes, and the mode of cell death, cells were seeded on glass coverslips.

Analysis of intracellular uptake and localization of liposomes: The cells were incubated with NBD-labeled cationic, neutral, or anionic liposomes at a concentration of 50 μM lipids for 24 h at 37 °C in 5% CO_2. After washing with phosphate-buffered saline (PBS) solution, the cells were replaced with fresh medium and uptake of liposomes was monitored by fluorescence microscopy. For analysis of the uptake mechanism of liposomes, the cells were pre-incubated at 37 °C or 4 °C without CO_2 for 30 min before liposome treatment. After incubation with NBD-labeled cationic liposomes at 37 °C or 4 °C for 1 h, the cells were washed with PBS and mounted in Permafluor (Beckman Coulter Inc.). Fluorescence images were obtained by using the LSM 410. The localization of liposomes was assayed by using rhodamine B-labeled cationic liposomes and LysoTracker Green (Molecular Probes). After incubation with liposomes for 1 h at 37 °C, the cells were washed with PBS and further cultured for 6 h, after which fresh medium was supplied. To visualize the lysosome, the cells were treated with LysoTracker Green (500 nM) by its addition to the culture medium for 1 h before observation. After washing with PBS, the cells were mounted in Permafluor and observed by using the LSM 410.

Photodynamic activity experiments and cell staining with PI and FITC-conjugated annexin V: The cells were incubated with $LMIC_{60}$ or $LMIC_{70}$ ([fullerene] = 5 μM) for 24 h in the dark at 37 °C in 5% CO_2. After incubation, the cells were washed with PBS and exposed to light, after which fresh medium was supplied. Photoirradiation was carried out under 19 mW cm^{-2} light power (λ = 350–500 nm) or 57 mW cm^{-2} light power (λ = 400–740 nm) at the cell level at 35 °C. To visualize the nonviable cells, the cells were stained with PI (1 μg mL^{-1}; Sigma-Aldrich) for 10 min at room temperature following $LMIC_{60}$ or $LMIC_{70}$ treatment, photoirradiation, and 24 h incubation after photoirradiation. After washing with PBS, the cells were replaced with fresh medium and monitored by fluorescence microscopy. For analysis of the mode of cell death, the cells were stained with PI (1 μg mL^{-1}) and FITC-conjugated annexin V (0.5 μg mL^{-1}; BioVision) according to the manufacturer's instructions after photoirradiation. After staining with PI and annexin V, the cells were mounted in Permafluor and observed by fluorescence microscopy.

Acknowledgement

This work was supported by Grants-in-Aid for Scientific Research from the Ministry of Education, Culture, Sports, Science and Technology, Japan.

[1] a) T. J. Dougherty, C. J. Gomer, B. W. Henderson, G. Jori, D. Kessel, M. Korbelik, J. Moan, Q. Peng, *J. Natl. Cancer Inst.* **1998**, *90*, 889–905; b) H. Kato, *J. Photochem. Photobiol. B* **1998**, *42*, 96–99.

[2] a) R. Bernstein, F. Prat, C. S. Foote, *J. Am. Chem. Soc.* **1999**, *121*, 464–465; b) Y. Yamakoshi, N. Umezawa, A. Ryu, K. Arakane, N. Miyata, Y. Goda, T. Masumizu, T. Nagano, *J. Am. Chem. Soc.* **2003**, *125*, 12803–12809; c) L. Xiao, H. Takada, K. Maeda, M. Haramoto, N. Miwa, *Biomed. Pharmacother.* **2005**, *59*, 351–358.

[3] a) A. Ikeda, T. Hatano, M. Kawaguchi, H. Suenaga, S. Shinkai, *Chem. Commun.* **1999**, 1403–1404; b) A. Ikeda, A. Ejima, K. Nishiguchi, J. Kikuchi, T. Matsumoto, T. Hatano, S. Shinkai, M. Goto, *Chem. Lett.* **2005**, *34*, 308–309; c) A. Ikeda, T. Sato, K. Kitamura, K. Nishiguchi, Y. Sasaki, J. Kikuchi, T. Ogawa, K. Yogo, T. Takeya, *Org. Biomol. Chem.* **2005**, *3*, 2907–2909; d) A. Ikeda, Y. Doi, K. Nishiguchi, K. Kitamura, M. Hashizume, J. Kikuchi, K. Yogo, T. Ogawa, T. Takeya, *Org. Biomol. Chem.* **2007**, *5*, 1158–1160; e) A. Ikeda, Y. Doi, M. Hashizume, J. Kikuchi, T. Konishi, *J. Am. Chem. Soc.* **2007**, *129*, 4140–4141; f) M. Akiyama, A. Ikeda, T. Shintani, Y. Doi, J. Kikuchi, T. Ogawa, K. Yogo, T. Takeya, N. Yamamoto, *Org. Biomol. Chem.* **2008**, *6*, 1015–1019.

[4] a) Y. Tabata, Y. Ikada, *Pure Appl. Chem.* **1999**, *71*, 2047–2053; b) S. Bosi, T. Da Ros, G. Spalluto, M. Prato, *Eur. J. Med. Chem.* **2003**, *38*, 913–923; c) E. Nakamura, H. Isobe, *Acc. Chem. Res.* **2003**, *36*, 807–815.

[5] T. Hamano, K. Okuda, T. Mashino, M. Hirobe, K. Arakane, A. Ryu, S. Mashiko, T. Nagano, *Chem. Commun.* **1997**, 21–22.

[6] A. Ikeda, T. Irisa, T. Hamano, T. Kitahashi, Y. Sasaki, M. Hashizume, J. Kikuchi, T. Konishi, S. Shinkai, *Org. Biomol. Chem.* **2006**, *4*, 519–523.

[7] Y. N. Yamakoshi, T. Yagami, K. Fukuhara, S. Sueyoshi, N. Miyata, *J. Chem. Soc. Chem. Commun.* **1994**, 517–518.

[8] a) H. Hungerbühler, D. M. Guldi, K.-D. Asmus, *J. Am. Chem. Soc.* **1993**, *115*, 3386–3387; b) R. V. Bensasson, E. Bienvenue, M. Dellinger, S. Leach, P. Seta, *J. Phys. Chem.* **1994**, *98*, 3492–3500.

[9] a) T. Andersson, K. Nilsson, M. Sundahl, G. Westman, O. Wennerström, *J. Chem. Soc. Chem. Commun.* **1992**, 604–606; b) K. Komatsu, K. Fujiwara, Y. Murata, T. Braun, *J. Chem. Soc. Perkin Trans. 1* **1999**, 2963–2966.

[10] a) A. Ikeda, T. Hatano, S. Shinkai, T. Akiyama, S. Yamada, *J. Am. Chem. Soc.* **2001**, *123*, 4855–4856; b) A. Ikeda, T. Hatano, T. Konishi, S. Shinkai, *Tetrahedron* **2003**, *59*, 3537–3540; c) T. Konishi, A. Ikeda, M. Asai, T. Hatano, S. Shinkai, M. Fujitsuka, O. Ito, Y. Tsuchiya, J. Kikuchi, *J. Phys. Chem. B* **2003**, *107*, 11261–11266; d) A. Ikeda, A. Ejima, K. Nishiguchi, J. Kikuchi, T. Matsumoto, T. Hatano, S. Shinkai, M. Goto, *Chem. Lett.* **2005**, *34*, 308–309.

[11] *Liposomes: A Practical Approach* (Eds.: V. P. Torchilin, W. Weissig), 2nd ed., Oxford University Press, Oxford (UK), **2003**.

[12] a) Y. Matsumura, H. Maeda, *Cancer Res.* **1986**, *46*, 6387; b) H. Maeda, L. Seymour, Y. Miyamoto, *Bioconjugate Chem.* **1992**, *3*, 351.

[13] C. R. Miller, B. Bondurant, S. D. McLean, K. A. McGovern, D. F. O'Brien, *Biochemistry* **1998**, *37*, 12875–12883.

[14] M. van Engeland, L. J. W. Nieland, F. C. S. Ramaekers, B. Schutte, C. P. M. Reutelingsperger, *Cytometry* **1998**, *31*, 1–9.

[15] K. R. Weishaupt, C. J. Gomer, T. J. Dougherty, *Cancer Res.* **1976**, *36*, 2326.

[16] B. A. Lindig, M. A. J. Rodgers, A. P. Schaap, *J. Am. Chem. Soc.* **1980**, *102*, 5590–5593.

[17] We attempted to generate $^1O_2$ by using $LMIC_{60}$ and $LMIC_{70}$ of **1+2**, but the absorbance of $LMIC_{60}$ and $LMIC_{70}$ of **1+2** increased as a result of light scattering several hours after the addition of ADPA. The reason for this is considered to be that anionic ADPA induced the self-assembly of cationic liposomes by electrostatic interactions. Therefore, we used zwitterionic $LMIC_{60}$ and $LMIC_{70}$ of **1**.

[18] Y. Murakami, A. Nakano, A. Yoshimatsu, K. Uchitomi, Y. Matsuda, *J. Am. Chem. Soc.* **1984**, *106*, 3613–3623.

[19] The ^{1}H NMR spectroscopic method was used to confirm that all C_{60} was transferred from the γ-CD cavity to lipid membranes to yield vesicle-incorporated C_{60}. ^{1}H NMR spectra for all LMI [60]fullerenes show that the peaks at δ = 5.41 ppm assignable to the aggregation of the C_{60}•γ-CD complex by itself did not appear and that the peaks assignable to the C_{60}•γ-CD complex (δ = 4.19 and 5.05 ppm) disappeared by heating at 80 °C for 2 h after addition of the **1+2**, **1**, and **1+3** vesicles.

Received: June 5, 2008
Published online: August 12, 2008

